

Storage capacity of networks with discrete synapses and sparsely encoded memoriesYu Feng ^{1,*} and Nicolas Brunel ^{1,2}¹*Department of Physics, Duke University, Durham, North Carolina 27710, USA*²*Department of Neurobiology, Duke University, Durham, North Carolina 27710, USA*

(Received 13 December 2021; accepted 11 March 2022; published 16 May 2022)

Attractor neural networks are one of the leading theoretical frameworks for the formation and retrieval of memories in networks of biological neurons. In this framework, a pattern imposed by external inputs to the network is said to be learned when this pattern becomes a fixed point attractor of the network dynamics. The storage capacity is the maximum number of patterns that can be learned by the network. In this paper, we study the storage capacity of fully connected and sparsely connected networks with a binarized Hebbian rule, for arbitrary coding levels. Our results show that a network with discrete synapses has a similar storage capacity as the model with continuous synapses, and that this capacity tends asymptotically towards the optimal capacity, in the space of all possible binary connectivity matrices, in the sparse coding limit. We also derive finite coding level corrections for the asymptotic solution in the sparse coding limit. The result indicates the capacity of networks with Hebbian learning rules converges to the optimal capacity extremely slowly when the coding level becomes small. Our results also show that in networks with sparse binary connectivity matrices, the information capacity per synapse is larger than in the fully connected case, and thus such networks store information more efficiently.

DOI: [10.1103/PhysRevE.105.054408](https://doi.org/10.1103/PhysRevE.105.054408)**I. INTRODUCTION**

It is widely believed that memories are stored in the brain through synaptic modifications in an activity-dependent way. This idea has been implemented in attractor neural network (ANN) models, where the connectivity strength between neurons is determined by Hebbian synaptic plasticity rules [1,2]. In this framework, a pattern is said to be learned if it becomes a fixed point attractor of the network dynamics. An extensively studied question is as follows: How many patterns can be stored in such networks? Classical studies of memory modeling synapses as continuous variables in networks of binary neurons have shown that such networks can store a number of uncorrelated random patterns p that scale linearly that network size $p_{\max} = \alpha_c N$ where α_c is of order 1 in the large N limit [2–4]. However, there is evidence suggesting that synapses in brain structures involved in memory, such as the hippocampus and neocortex, are more digital than analog [5–8].

A number of studies have addressed the question of the storage capacity of networks with discrete synapses. Krauth and Mézard showed that networks can potentially have a large capacity when all synapses are required to be binary [9], using Gardner’s approach [4], with an upper bound for capacity $\alpha_{c\max} = 0.83$ discrete synapses, instead of $\alpha_{c\max} = 2$ for continuous synapses. Sompolinsky studied the storage capacity of a network with a specific binarized Hebbian rule [10,11], and showed its capacity is remarkably close to the capacity of the Hopfield network [1], whose synapses are continuous variables ($\alpha_c = 0.10$ instead of 0.14). However, these authors only

studied the unbiased case, in which the coding level f (i.e., fraction of active neurons in a pattern) is 0.5, while neuronal activity in areas involved in memory is typically very sparse (e.g., [12]), for instance, the coding level in the human medial temporal lobe has been estimated to be around 1% [13]. The upper bound for capacity in networks with arbitrary coding levels and discrete synapses was computed by Gutfreund and Stein [14]. The capacity in networks with Hebbian plasticity and binary synapses has only been computed in the unbiased case, and the capacity for arbitrary coding levels remains an open question. In this paper, we generalized Sompolinsky’s calculation on the Hopfield model with binary synapses when coding level $f = 0.5$, to the model with fully connected or sparsely connected binary synaptic connectivity with arbitrary coding levels. Our results show that the network with binarized Hebbian rule has a similar capacity as the model with continuous synapses for any coding level, and that this capacity tends asymptotically towards the optimal capacity obtained by Gutfreund and Stein [14], in the space of all possible binary connectivity matrices. Our results also show that a network with sparse binary connectivity can have a larger information capacity per synapse than a fully connected network, and thus can allow a network to store information more efficiently.

II. RESULTS**A. Storage capacity of fully connected network with binary synapses**

We consider a fully connected neural network with N binary (0,1) neurons. The activity of neuron i ($i = 1, \dots, N$) is described by a binary variable $V_i = 0, 1$. Each neuron is connected to other neurons through the connectivity matrix W . The activity of neuron i at time t is determined by the

*Corresponding author: yu.feng707@duke.edu

asynchronous update rule (see Appendix 6, for details):

$$V_i(t+1) = \Theta[h_i(t) - \theta], \quad (1)$$

where

$$h_i(t) = \sum_{j \neq i}^N W_{ij} V_j(t) \quad (2)$$

is the local field, defined as the total input of neuron i , where θ is an activation threshold (constant independent of V_i), and Θ is the Heaviside function. We also consider in the Appendix a more general case of dynamics with stochastic updates characterized by a temperature T , but we focus in the main text in the zero temperature, deterministic limit.

The storage capacity of the network whose dynamics is defined by Eqs. (1) and (2) is determined by the connectivity matrix W . This connectivity matrix W depends on p random uncorrelated patterns $\tilde{\eta}^\mu$, $\mu = 1, \dots, p$, that are described by independent Bernoulli random variables:

$$P(\eta_i^\mu) = f \delta_{(\eta_i^\mu, 1)} + (1-f) \delta_{(\eta_i^\mu, 0)}, \quad (3)$$

where δ is the Kronecker delta function, and where f is the coding level (the fraction of active neurons). The storage capacity α is defined as the maximal number of stored patterns p divided by the network size N , $\alpha = p/N$.

In this paper, we construct connectivity matrix W from the patterns $\tilde{\eta}^\mu$ using a ‘‘clipped’’ learning rule:

$$W_{ij} = \frac{\sqrt{p}}{N} F \left(\frac{1}{f(1-f)\sqrt{p}} \sum_{\mu=1}^p (\eta_i^\mu - f)(\eta_j^\mu - f) \right), \quad (4)$$

where F is given by

$$F(x) = \sqrt{\frac{\pi}{2}} \text{sign}(x), \quad (5)$$

where the prefactor $\sqrt{\pi/2}$ is used for convenience. Thus, W_{ij} is only allowed to take two distinct values. With the nonlinear function $F(x)$ given by Eq. (5), W_{ij} can be positive or negative. In neurobiological networks, synaptic weights are sign constrained, and their sign depends on whether the presynaptic neuron is excitatory or inhibitory. The network with the connectivity matrix given by Eqs. (4) and (5) leads to local fields of the form

$$h_i = \sum_j W_{ij} V_j = \frac{\sqrt{2\pi p}}{N} \sum_j \Theta(x_{ij}) V_j - \sqrt{\frac{\pi p}{2}} \frac{1}{N} \sum_j V_j, \quad (6)$$

where $\Theta(x)$ is the Heaviside function, and x_{ij} is the argument of F in Eq. (4). Equation (6) shows that the network is equivalent to a purely excitatory network with binary weights [the first term in the right-hand side of Eq. (6)] with an instantaneous linear inhibition [the second term in the right-hand side of Eq. (6)].

Notice also that when $F(x) = x$, Eq. (4) yields the learning rule in the model of Tsodyks and Feigel'man (TF) [2], where W_{ij} is a continuous variable. Therefore, we can interpret the learning rule of Eq. (4) as first learning patterns $\tilde{\eta}^\mu$ using the TF learning rule, and then clipping the weight into discrete values at the end of the learning phase. In the following, we call this model the clipped Tsodyks-Feigel'man (CTF) model.

The nonlinearity of $F(x)$ in Eq. (5) makes the storage capacity more difficult to calculate than the one of a network with a linear learning rule. In 1986, Sompolinsky introduced a method to compute the storage capacity of Hopfield networks with nonlinear learning rules [10,11]. In particular he showed that in the large N limit, these networks are equivalent to a linear learning rule with an added random Gaussian noise,

$$W_{ij} = \frac{J}{Nf(1-f)} \sum_{\mu}^p (\eta_i^\mu - f)(\eta_j^\mu - f) + \delta_{ij}, \quad (7)$$

where J is an embedding strength, and δ_{ij} is a random symmetric Gaussian matrix. Both J and the variance of the random Gaussian matrix $\Delta_0^2 = N \langle \delta_{ij}^2 \rangle / (J^2 \alpha)$ can be calculated as a function of $F(x)$ [11]. For $F(x)$ given by Eq. (5), the embedding strength J and Δ_0^2 are given by (see details in the Appendix)

$$J = 1, \quad \Delta_0^2 = \frac{\pi}{2} - 1. \quad (8)$$

1. Calculation of the storage capacity for arbitrary coding level f

To compute the storage capacity of a network with a learning rule given by Eq. (7), we use standard methods and introduce the Hamiltonian

$$H = \frac{1}{2} \sum_{i \neq j} W_{ij} V_i V_j + \theta \sum_i V_i, \quad (9)$$

where W_{ij} is given Eq. (7). The typical free energy of the system can be derived using the replica method [3,10,15]. The calculation allows us to derive order parameters characterizing the system (such as the overlap of network state with stored patterns), and its storage capacity. Using a replica symmetric ansatz, the free energy of the system can be characterized by five order parameters m, Q, q, R, r , where

$$\begin{aligned} m &= \frac{1}{N} \sum_i \tilde{\eta}_i^1 V_i, \\ Q &= \frac{1}{N} \sum_i V_i, \\ q &= \frac{1}{N} \sum_i V_i^2, \end{aligned} \quad (10)$$

and where R and r are conjugate variables of Q and q , and are defined by Eqs. (A19) in the Appendix 2. The order parameter m measures the retrieval quality of a pattern stored in memory. Solutions with $\tilde{m} \equiv \frac{m}{f(1-f)} \sim 1$ represent ‘‘retrieval states’’ in which the network goes to a fixed point close to one of the stored patterns. Solutions with $\tilde{m} = 0$ correspond to no retrieval. The order parameters Q and q represent the average neural activity and square of neural activity of the network (see Appendix 2, for more details). The mean-field equations of the system are obtained using a saddle point method. The full equations are given by Eq. (A24) in Appendix 2, for arbitrary coding levels and temperature. In the zero-temperature limit, the equations simplify to the following

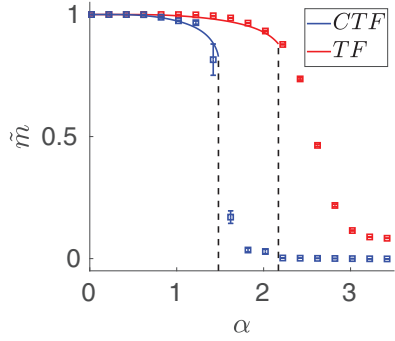


FIG. 1. Overlap as a function of storage load α for the Tsodyks-Feigl' man model (TF) and the clipped Tsodyks-Feigl' man model (CTF), for $f = 0.02$. The solid lines represent the theoretical prediction and squares represent the simulation results with a network of size $N = 4000$ (mean and standard deviation computed over five independent realizations). Dashed lines mark the storage capacity for CTF and TF. For both models, the neuronal activity threshold θ is chosen as the one that optimizes capacity. For the parameters chosen here ($f = 0.02$), $\tilde{\theta} \equiv \theta/f \approx 0.6$.

set of equations:

$$\begin{aligned}
 \tilde{m} &= \Phi(a_1) - \Phi(a_2), \\
 \tilde{r} &= f\Phi(a_1) + (1-f)\Phi(a_2), \\
 a_1 &= \frac{\tilde{\theta} - (1-f)\tilde{m} - Y}{\sqrt{\tilde{r}\alpha(1 + \Delta_0^2(1-C)^2)}}, \\
 a_2 &= \frac{\tilde{\theta} + f\tilde{m} - Y}{\sqrt{\tilde{r}\alpha(1 + \Delta_0^2(1-C)^2)}}, \\
 Y &= \frac{\alpha C f}{2(1-C)} + \frac{1}{2}\alpha C f \Delta_0^2, \\
 C &= \frac{f}{2\pi\alpha\tilde{r}}(f e^{-a_1^2/2} + (1-f)e^{-a_2^2/2}), \quad (11)
 \end{aligned}$$

where $\tilde{m} = m/f(1-f)$, $\tilde{\theta} = \theta/f$, $\Delta_0^2 = \Delta^2/\alpha$, and $\Phi(x) = \int_x^\infty Dz$.

Once f , α , θ are given, Eq. (11) can be solved numerically to obtain the order parameters, including the rescaled overlap with the retrieved pattern \tilde{m} . Figure 1 shows \tilde{m} as a function of α for both TF and CTF models for $f = 0.02$. The figure shows that analytical results are in good agreement with simulations, using a network with 4000 neurons. The maximal capacity of the network α_c is given by the largest value of α for which there exist retrieval states (i.e., states with nonzero \tilde{m}), optimized over the threshold θ . Figure 1 shows that the maximal capacity of the CTF model is lower than the one of the TF model, as expected, but only by a factor of about 1.5. This maximal capacity α_c is plotted as a function of f in Fig. 2(a).

2. Sparse coding limit

In the biologically relevant sparse coding limit $f \rightarrow 0$, the mean-field equation (A25) takes a rather simple

form:

$$\begin{aligned}
 \tilde{m} &= \Phi\left(\frac{\tilde{\theta} - \tilde{m}(1-f)}{\sqrt{\tilde{r}\alpha(1 + \Delta_0^2)}}\right) - \Phi\left(\frac{\tilde{\theta} + \tilde{m}f}{\sqrt{\tilde{r}\alpha(1 + \Delta_0^2)}}\right), \\
 \tilde{r} &= f\Phi\left(\frac{\tilde{m}f}{\sqrt{\tilde{r}\alpha(1 + \Delta_0^2)}}\right) + (1-f)\Phi\left(\frac{\tilde{\theta}}{\sqrt{\tilde{r}\alpha(1 + \Delta_0^2)}}\right), \quad (12)
 \end{aligned}$$

where $\tilde{\theta} = \theta/f$ is a rescaled threshold, $\tilde{r} = r/f^2$, and $\Phi(x) = \int_x^\infty Dz$ is the complementary cumulative distribution function of the standard Gaussian distribution.

With additional analysis (see details in Appendix 3), we find that the maximum capacity in this limit is obtained when $\tilde{\theta} \sim 1$, and the maximum capacity is

$$\alpha_c \simeq \frac{1}{\pi f |\ln f|}, \quad (13)$$

which can be compared with the capacity of TF model obtained by [2] $\alpha_c \simeq 1/(2f |\ln f|)$. Thus, the two capacities differ by a factor $\pi/2 \sim 1.57$. We next address the question of how close this capacity is to an upper bound in the space of all possible binary connectivity matrices. This upper bound was computed by Gutfreund and Stein [14] for arbitrary coding levels. The $f \rightarrow 0$ behavior could not be determined in a simple form in that paper; however, it was shown that the upper bound must be smaller or equal than $1/(\pi f |\ln f|)$. Our asymptotic result, Eq. (13), indicates that the upper bound for binary connectivity matrices is indeed asymptotically $1/(\pi f |\ln f|)$, and thus the clipped TF model becomes asymptotically optimal in the sparse coding limit. This is similar to what happens in networks with continuous synapses, for which it was shown that the storage capacity of the TF model tends to the upper bound of storage capacity obtained by Gardner [4], in the space of all continuous synaptic matrices in the sparse coding limit. Thus, in spite of their remarkable simplicity, both TF and CTF models provide close to optimal learning rules for models with continuous and discrete weights, respectively. For convenience, we summarize the storage capacity of different models in Table I [1,2,4,9,10].

3. Leading correction to sparse coding limit

We can see that the capacities of networks with Hebbian rules in the unbiased case ($f = 0.5$) are much smaller than the corresponding upper bounds, while they converge to the corresponding upper bounds in the sparse coding limit. However, solving numerically mean-field equation (A25) for finite coding level f , we find that the capacities of TF and CTF converge to the upper bounds extremely slowly [see Fig. 2(b)]. As shown in Fig. 2(b), the capacity of Hebbian rules is only around $1/3$ compared to their corresponding upper bounds when the coding level $f = 10^{-2}$. This is mainly because the optimal threshold $\tilde{\theta}$ approaches 1 extremely slowly when f decreases (for instance, for $f = 0.02$, $\tilde{\theta} \sim 0.6$). With additional analysis (see Appendix 3), we derived the leading

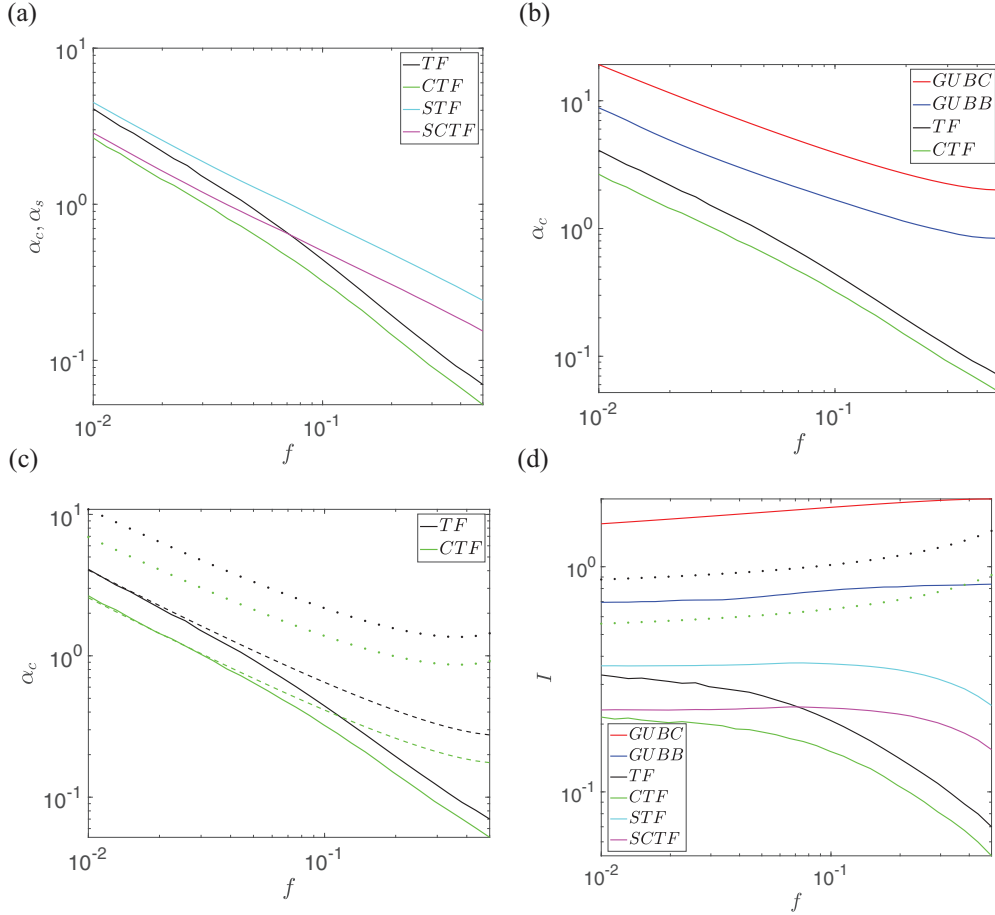


FIG. 2. Comparison between storage capacity of Hebbian rules and the respective upper bounds. GUBC: Gardner upper bound for networks with continuous weights [4]. GUBB: Gutfreund and Stein upper bound for networks with binary weights [14]. See more details about capacity upper bounds in Appendix 4. (a) Storage capacity of TF and CTF models as a function of coding level f . When $f \rightarrow 0$, both capacities increase as $1/f \ln(1/f)$. Cyan and magenta lines represent the storage capacity for a sparsely connected network with continuous weights (STF) and a network with binary weights (SCTF). The storage capacities of fully connected and sparsely connected networks converge when $f \rightarrow 0$. Notice that for fully connected network, storage capacity is defined as $\alpha_c = p/N$ while for the sparsely connected network, storage capacity is defined as $\alpha_s = p/cN$, where $c \ll 1$. (b) Comparison between storage capacity and upper bounds as a function of coding level f . Even at $f = 10^{-2}$, for both TF and CTF models, the capacity is only around a third of the respective bounds, and thus the asymptotic solution (12) is approached very slowly. (c) Comparison between the numerical solution and asymptotic solutions. Solid lines are the numerical solutions of TF and CTF models, the dotted lines with the same color are the corresponding asymptotic solutions in the sparse coding limit [Eq. (13)], and dashed lines represent asymptotic solutions with finite coding level corrections [Eqs. (14) and (15)]. (d) Stored information per synapse as a function of coding level. When the coding level f goes to 0, the information stored in synapses increases but with an extremely slow rate for both TF and CTF models. Dotted lines represents stored information of asymptotic solutions in the sparse coding limit (i.e., $I[\alpha = (2f|\ln f|)^{-1}]$ for continuous weights case and $I[\alpha = (\pi f|\ln f|)^{-1}]$ for binary weights case).

correction to the asymptotic solution at the finite coding level:

$$\alpha_c \simeq \frac{\tilde{\theta}_{\text{opt}}^2}{\pi f |\ln f|}, \quad (14)$$

TABLE I. Comparison between the storage capacity of Hebbian rules and upper bounds computed using Gardner approach.

	Capacity of Hebbian rule	Upper bound
$f = 0.5$, continuous W_{ij}	~ 0.14	2
$f = 0.5$, binary W_{ij}	~ 0.1	~ 0.83
$f \rightarrow 0$, continuous W_{ij}	$(2f \ln f)^{-1}$	$(2f \ln f)^{-1}$
$f \rightarrow 0$, binary W_{ij}	$(\pi f \ln f)^{-1}$	$(\pi f \ln f)^{-1}$

where the optimal threshold $\tilde{\theta}_{\text{opt}}$ is obtained by solving the equation

$$\frac{2\tilde{\theta}_{\text{opt}}^2 |\ln(1 - \tilde{\theta}_{\text{opt}})|}{(1 - \tilde{\theta}_{\text{opt}})^2} = |\ln f|. \quad (15)$$

Notice that when coding level $f \rightarrow 0$, $\tilde{\theta}_{\text{opt}} \rightarrow 1$ and Eq. (14) recovers the asymptotic scaling of Eq. (13). The asymptotic solutions (13) and (14) are compared in Fig. 2(c), and we can see that Eq. (14) agrees with the numerical solutions very well when the coding level f is small. This result indicates that, in the biological sparse coding limit (i.e., coding level is small but finite), the capacities of models with Hebbian rules are still notably smaller than the maximal capacities, in the space of all possible connectivity matrices.

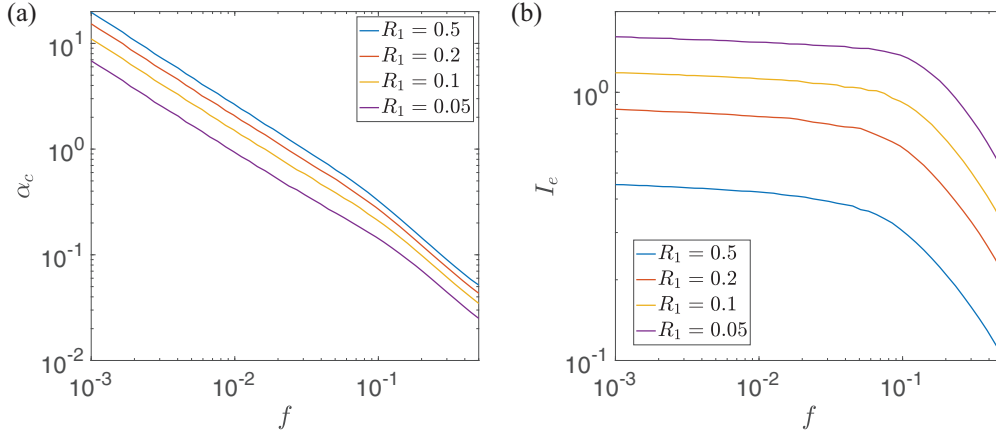


FIG. 3. Storage capacity and information capacity for a network with sparse excitatory binary connections. (a) Storage capacity as a function of connection probability R_1 and coding level f . The storage capacity decreases when R_1 decreases. (b) Information capacity per active synapse, as a function of f and R_1 . The information per synapse I_e increases when f and R_1 decrease. This indicates that for learning rule equations (4) and (20), both sparse coding and sparse connectivity can improve the coding efficiency of the network. This result also indicates that the network can have an optimal R_1 to balance storage capacity and coding efficiency.

While the storage capacity in terms of numbers of patterns stored per synapse diverges in the sparse coding limit, the information stored per pattern decreases in that limit since it is proportional to the binary entropy of f . As a result, the total information stored per synapse remains finite in the sparse coding limit, both in the TF model [2] and in the corresponding Gardner bound [4]. Figure 2(d) shows the information capacity in bits per synapse for different models as a function of f ,

$$I = -\frac{\alpha}{\ln 2} [f \ln f + (1-f) \ln(1-f)]. \quad (16)$$

We find that when the coding level f decreases, the information capacity of TF and CTF increases quickly, while the corresponding upper bounds decrease slowly. When f goes to 0, the information capacity I of TM and CTM further increase and eventually converge to the optimal information capacity, but the convergence rate is extremely low.

B. Storage capacity of sparsely connected network with binary synapses

Cortical networks are characterized by low connection probabilities between neurons (e.g., [16]). In the case we interpret the low synaptic efficacy state to be zero, the network we have studied so far has a 50% connection probability, much higher than observed connection probabilities in cortex, which are of order 10% for excitatory neurons at short distances ($<100 \mu\text{m}$). This motivates the study of networks with sparser connectivity. Here, we study two cases: one in which sparse connectivity is uncorrelated with learning, and the other one where sparse connectivity is an outcome of learning with a high synaptic threshold.

1. Sparse connectivity uncorrelated with learning

We first consider the case where learning occurs on top of a sparse random Erdos-Renyi “structural” connectivity matrix,

$$W_{ij} = \frac{c_{ij}\sqrt{p}}{Nc} F\left(\frac{1}{f(1-f)\sqrt{p}} \sum_{\mu=1}^p (\eta_i^\mu - f)(\eta_j^\mu - f)\right), \quad (17)$$

where $F(x)$ is the same as the clipped function (5) for fully connected case, and $c_{ij} = 1, 0$ is a random binary matrix, with

$$P(c_{ij}) = c\delta_{(c_{ij},1)} + (1-c)\delta_{(c_{ij},0)}, \quad (18)$$

where $0 < c \ll 1$ is the connection probability. The storage capacity of learning rule (17) can be calculated similarly as the model in [17] in the sparse connectivity limit $c \ll 1$, and the mean-field equations for finite coding level f are given as (see details in the Appendix 5)

$$\begin{aligned} \tilde{m} &= \Phi\left(\frac{\tilde{\theta} - \tilde{m}(1-f)}{\sqrt{\alpha_s q(1+\Delta_0^2)}}\right) - \Phi\left(\frac{\tilde{\theta} + \tilde{m}f}{\sqrt{\alpha_s q(1+\Delta_0^2)}}\right), \\ q &= f\Phi\left(\frac{\tilde{\theta} - \tilde{m}(1-f)}{\sqrt{\alpha_s q(1+\Delta_0^2)}}\right) + (1-f)\Phi\left(\frac{\tilde{\theta} + \tilde{m}f}{\sqrt{\alpha_s q(1+\Delta_0^2)}}\right), \end{aligned} \quad (19)$$

where $\alpha_s = p/cN$ and where other order parameters are defined in Eq. (10). The numerical solution of Eq. (19) is compared with the fully connected case in Fig. 2(a). In the sparse coding case, the mean-field (19) coincides with the mean field (12), as expected [17]. We see that the capacity, in terms of number of patterns stored divided by number of connections per neuron, is larger in the sparsely connected case than in the fully connected case, as expected from previous results in networks with continuous synapses [17,18].

2. Sparse connectivity induced by learning

In this section, we consider the case where sparse connectivity is obtained by adding a threshold to the clipped function. Here we generalize the clipped function (5) to

$$F_T(x) = \sqrt{2\pi} [\Theta(x-T) - M], \quad (20)$$

where M is given by

$$M = \frac{1}{\sqrt{2\pi}} \int_{-\infty}^{\infty} \Theta_T(x) e^{-x^2/2} dx, \quad (21)$$

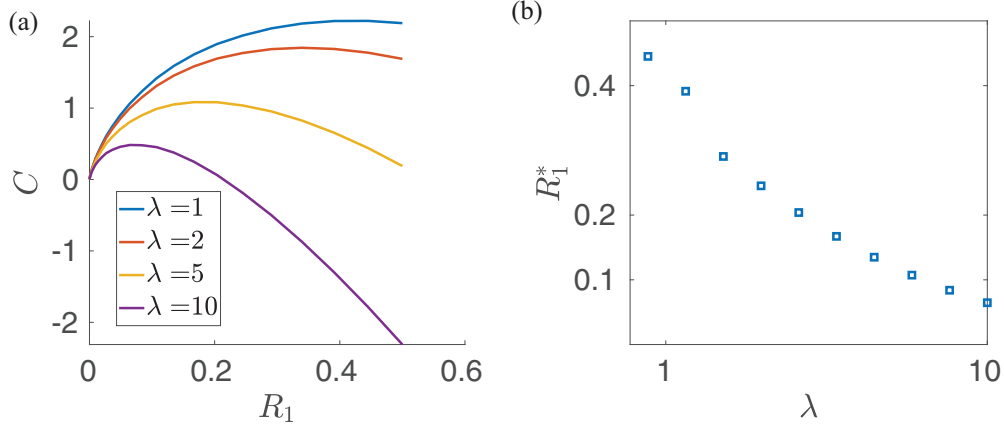


FIG. 4. Connection probability that optimizes capacity subject to a synapse maintenance cost λ . (a) Cost function C as a function of R_1 and λ . (b) Optimal connection probability R_1^* for different λ . We can see that the more costly synaptic maintenance is, the sparser the resulting connectivity. In both (a) and (b), coding level is set to be $f = 0.01$.

where $\Theta_T(x) = \Theta(x - T)$, and T is the threshold that can be used to increase the sparseness of network connectivity, interpreting the low synaptic state as a 0 state. With such a connectivity matrix, the connection probability R_1 is given by

$$R_1 = \frac{1}{2} \left[1 - \operatorname{erf} \left(\frac{T}{\sqrt{2}} \right) \right]. \quad (22)$$

In this case, the embedding strength J and additional noise introduced by clipped function (20), $\Delta_0^2 = N \langle \delta_{ij}^2 \rangle / J^2 \alpha$, are

$$J = e^{-T^2}, \quad \Delta_0^2 = \frac{\pi}{2} e^{T^2} \left[1 - \operatorname{erf} \left(\frac{T}{\sqrt{2}} \right) \right]^2 - 1. \quad (23)$$

Notice that the noise strength $\Delta_0^2 = N \langle \delta_{ij}^2 \rangle / J^2 \alpha$ is an increasing function of T . The storage capacity of the learning rule (4,20) is determined by mean field (12) for a given connection probability R_1 and coding level f . As shown in Fig. 3(a), the storage capacity α_c decreases when the threshold increases, and consequently the connection probability R_1 decreases. Unsurprisingly, the storage capacity decreases as the fraction of nonzero synapses decreases. However, storing information with a smaller number of synapses also carries benefits in terms of efficiency of information storage.

To quantify this efficiency, we calculate the information stored in the network per nonzero synapse I_e :

$$I_e = -\frac{\alpha}{R_1 \ln 2} [f \ln f + (1-f) \ln(1-f)]. \quad (24)$$

The relation between I_e , R_1 , and f is shown in Fig. 3(b). We see that the information capacity per synapse increases when the excitatory connectivity becomes more sparse. This is mainly because we only keep connections for which the Hebbian term [i.e., the argument of the clipping function F in Eq. (20)] is large. In this way, the network can encode information more efficiently when excitatory connections become sparse. Note that maximizing storage capacity subject to a constraint of minimizing the fraction of active synapses would lead to an optimal connection probability R_1^* , whose precise value would depend on the cost of maintenance of an active synapse. One can define a cost function $C = \alpha - \lambda R_1$, where the second term represents the cost of maintenance of active

synapses. For a given λ , we can obtain R_1^* that maximize C . As shown in Fig. 4(b), the more costly synaptic maintenance is, the sparser the resulting connectivity. And the optimal connection probability $R_1^* \sim 0.1$ when $\lambda \sim 10$.

III. DISCUSSION

We have calculated the storage capacity of an attractor neural network endowed with binary synaptic weights at arbitrary coding levels. Our results show that a network with a binarized Hebbian learning rule has a capacity that is close to the capacity of a network with continuous weights at any coding level since the decrease in capacity is only about 1.5 compared to continuous weights. Our results generalize the results obtained by Sompolinsky for a coding level $f = 0.5$ [11], to arbitrary coding levels. Furthermore, our analysis shows that the storage capacity of CTF tends in the sparse coding limit to the upper bound of storage capacity, in the space of all possible binary connectivity matrices. We also provide a finite coding level correction for this asymptotic solution, and the results indicate the capacities of TF and CTF converge extremely slowly to the optimal capacity when the coding level decreases since the corrections are of order $1/\sqrt{\ln(1/f)}$. In particular, for $f = 0.01$ [13], the capacity of the clipped model is only about a third of the upper bound. Our results also show that sparse connectivity matrices can allow these networks to have a larger information capacity per synapse and thus encode information more efficiently.

The binary connectivity matrices used in this paper were constructed using a clipped function whose argument is an analog variable containing information about all stored patterns. This assumes that the synapse can store continuous information during the learning phase, before binarizing this information. An alternative scenario is that the synapse is required to be discrete during all learning phases. Tsodyks, Amit, and Fusi studied models with discrete synapses under an online learning setting in which synapses only have information about the currently shown pattern to make a transition between states. They showed that this leads to a drastic decrease in storage capacity when the coding level is $f = 0.5$ [19–21] since in that case the total number of stored patterns

can scale at most as \sqrt{N} , implying a vanishing amount of information stored per synapse in the large N limit. Later work found that a storage capacity of order 1 bit/synapse can be recovered in the sparse coding limit [$f \sim \ln(N)/N$], even when synapses are required to be discrete during all phases of learning [21,22].

Another scenario studied by multiple authors consists in synapses with binary weights with multiple hidden states (describing, e.g., different configurations of protein interaction networks on the post-synaptic side) [23–26]. With appropriate structure of hidden states, such synapses can greatly extend the time for which synaptic connectivity can remain correlated with a pattern shown at a particular time. This scenario has been primarily studied using a signal-to-noise analysis quantifying the degree of correlation of the synaptic matrix with patterns presented to the network. To our knowledge, this scenario has never been implemented in attractor network models, and thus the storage capacity in these multistate models is still an open question. More experimental data will be necessary to understand which class of models best captures synaptic plasticity in neurobiological synapses.

ACKNOWLEDGMENTS

This work was supported by NIH R01MH115555.

APPENDIX

1. Calculation of J and Δ_0

To compute J and Δ_0 in Eq. (8) we use the same strategy as Sompolinsky [10,11]. We first calculate the average overlap between a given pattern and the local field when the network is retrieving that pattern. Let us denote $\tilde{\eta}_i^\mu = \eta_i^\mu - f$. For the learning rule given by Eq. (7), we have

$$\left\langle \tilde{\eta}_i^1 \sum_j \tilde{\eta}_j^1 W_{ij} \right\rangle = Jf(1-f). \quad (\text{A1})$$

Similarly, the average overlap for clipped learning rule (4) is

$$\begin{aligned} \left\langle \tilde{\eta}_i^1 \sum_j \tilde{\eta}_j^1 W_{ij} \right\rangle &= \frac{\sqrt{p}}{N} \left\langle \sum_j \tilde{\eta}_i^1 \tilde{\eta}_j^1 F \left(\frac{\sum_\mu \tilde{\eta}_i^\mu \tilde{\eta}_j^\mu}{\sqrt{p}f(1-f)} \right) \right\rangle \\ &= f(1-f) \langle xF(x) \rangle, \end{aligned} \quad (\text{A2})$$

where

$$x = \frac{\sum_\mu \tilde{\eta}_i^\mu \tilde{\eta}_j^\mu}{\sqrt{p}f(1-f)}. \quad (\text{A3})$$

In the large p limit, x becomes a random variable drawn from a standard Gaussian distribution $x \sim N(0, 1)$ according to the central limit theorem. Thus, from Eqs. (A1) and (A2), we obtain the embedding strength J as

$$J = \langle xF(x) \rangle. \quad (\text{A4})$$

In order to obtain the variance δ_{ij} of Eq. (7), we calculate the variance of synaptic weights for both linear and clipped learning rules. In the linear case, we have

$$N^2 \langle W_{ij}^2 \rangle = N^2 \frac{J^2}{f^2(1-f)^2 N^2} \left\langle \left(\sum_\mu \tilde{\eta}_i^\mu \tilde{\eta}_j^\mu \right)^2 \right\rangle$$

$$\begin{aligned} &= pJ^2 \left\langle \left(\sum_\mu \frac{\tilde{\eta}_i^\mu \tilde{\eta}_j^\mu}{f(1-f)\sqrt{p}} \right)^2 \right\rangle \\ &= N\alpha J^2. \end{aligned} \quad (\text{A5})$$

The $\langle \dots \rangle$ in Eq. (A5) goes to 1 when $p \rightarrow \infty$. For the clipped $F(x)$, the variance of the weights is

$$\begin{aligned} N^2 \langle W_{ij}^2 \rangle &= N^2 \frac{1}{N^2} p \left\langle F^2 \left(\sum_\mu \frac{\tilde{\eta}_i^\mu \tilde{\eta}_j^\mu}{f(1-f)\sqrt{p}} \right) \right\rangle \\ &= p \langle F^2(x) \rangle \\ &= N\alpha \tilde{J}^2, \end{aligned} \quad (\text{A6})$$

where we denote $\langle F^2(x) \rangle$ as \tilde{J}^2 . From Eqs. (A5) and (A6), we can see the additional noise introduced by a nonlinear $F(x)$ is

$$\langle \delta_{ij}^2 \rangle = \frac{\alpha}{N} (\tilde{J}^2 - J^2). \quad (\text{A7})$$

Let Δ_0^2 denote $N \langle \delta_{ij}^2 \rangle / J^2 \alpha$, we have

$$\Delta_0^2 = \left(\frac{\tilde{J}^2}{J^2} - 1 \right). \quad (\text{A8})$$

For $F(x)$ given by Eq. (5), we obtain the embedding strength and noise parameter as

$$J = 1, \quad \Delta_0^2 = \pi/2 - 1. \quad (\text{A9})$$

2. Storage capacity of the fully connected CTF model

The Hamiltonian for the learning rule (7) is

$$H = \frac{1}{2} \sum_{i \neq j} W_{ij} V_i V_j + \theta \sum_i V_i, \quad (\text{A10})$$

where W_{ij} is determined from Eqs. (7) and (A9). We can calculate the corresponding free energy by using the replica method (see, e.g., [2,3]). To compute the average logarithm of the partition function over the distribution of all random binary patterns $\langle \ln Z \rangle$ directly, we can use the relation

$$\langle \ln Z \rangle = \lim_{n \rightarrow 0} \frac{\langle Z^n \rangle - 1}{n}. \quad (\text{A11})$$

For the Hamiltonian in Eq. (A10), we have

$$\begin{aligned} \langle \langle Z^n \rangle \rangle &\propto \left\langle \left\langle \text{Tr}_{V^a} \exp \left[\frac{\beta J}{f(1-f)2N} \sum_{\mu a} \left(\sum_i \tilde{\eta}_i^\mu V_i^a \right)^2 \right. \right. \right. \\ &\quad \left. \left. \left. + \frac{\beta}{2} \sum_{ija} \delta_{ij} V_i^a V_j^a - \beta \theta \sum_{ia} V_i^a \right] \right\rangle \right\rangle, \end{aligned} \quad (\text{A12})$$

where $a = 1, \dots, n$ is the replica index and the double angular brackets mean the average over both V_i^a and η_i^μ . We are interested in the overlaps between the network state and the patterns stored in memory. We assume that the network has a macroscopic overlap with a single stored pattern ($\mu = 1$ the

one currently being retrieved by the network) and define the following order parameters:

$$m_a \equiv \frac{1}{N} \sum_i \tilde{\eta}_i^1 V_i^a, \quad m_{\mu a} \equiv \frac{1}{\sqrt{N}} \sum_i \tilde{\eta}_i^\mu V_i^a. \quad (\text{A13})$$

The partition function can be rewritten in terms of these order parameters as

$$\begin{aligned} \langle\langle Z^n \rangle\rangle \propto & \left\langle\left\langle \int \prod_{\mu a} dm_a^\mu \frac{\beta N}{2\pi} \exp \left(-\frac{\beta J N}{2f(1-f)} \sum_a m_a^2 + \frac{\beta J}{f(1-f)} \sum_a m_a \sum_i \tilde{\eta}_i^1 V_i^a \right. \right. \right. \\ & \left. \left. - \frac{\beta J}{2f(1-f)} \sum_{\mu a} (m_a^\mu)^2 + \frac{\beta J}{\sqrt{N}f(1-f)} \sum_{\mu a} m_a^\mu \sum_i \tilde{\eta}_i^\mu V_i^a + \frac{\beta}{2} \sum_{ija} V_i^a V_j^a \delta_{ij} - \beta \theta \sum_{ia} V_i^a \right) \right\rangle. \end{aligned} \quad (\text{A14})$$

The terms including η_i^μ and δ_{ij} in Eq. (A14) can be averaged:

$$\left\langle \exp \left(\frac{\beta J}{\sqrt{N}f(1-f)} \sum_{\mu a} m_a^\mu \sum_i \tilde{\eta}_i^\mu V_i^a \right) \right\rangle \propto \exp \left(\frac{\beta^2 J^2}{2Nf(1-f)} \sum_{i\mu ab} V_i^a V_j^a m_a^\mu m_b^\mu \right), \quad (\text{A15})$$

$$\left\langle \exp \left(\frac{\beta}{2} \sum_{ija} V_i^a V_j^a \delta_{ij} \right) \right\rangle \propto \exp \left[N\beta^2 J^2 \Delta^2 \sum_{ab} \left(\frac{1}{N} \sum_i V_i^a V_i^b \right) \left(\frac{1}{N} \sum_i V_i^a V_i^b \right) \right], \quad (\text{A16})$$

where $\Delta^2 = N\langle\delta_{ij}^2\rangle/J^2$. We then introduce the order parameters

$$Q_a = \frac{1}{N} \sum_i V_i^a, \quad q_{ab} = \frac{1}{N} \sum_i V_i^a V_i^b, \quad (\text{A17})$$

and use the integral representation of the δ function:

$$\delta \left(NQ_a - \sum_i V_i^a \right) = \int \frac{dR_a}{2\pi} e^{-R_a(NQ_a - \sum_i V_i^a)}, \quad \delta \left(Nq_{ab} - \sum_i V_i^a V_i^b \right) = \int \frac{dr_{ab}}{2\pi} e^{-r_{ab}(Nq_{ab} - \sum_i V_i^a V_i^b)}. \quad (\text{A18})$$

Combining Eqs. (A14)–(A18), the partition function can be written as

$$\langle\langle Z^n \rangle\rangle \propto \int \left(\prod_a dQ_a dR_a \right) \left(\prod_{a \neq b} dq_{ab} dr_{ab} \right) e^{-N\beta g(\beta, m, Q, q, R, r)}, \quad (\text{A19})$$

where

$$\begin{aligned} g = & \frac{J}{2f(1-f)} \sum_a m_a^2 + \theta \sum_a Q_a - \frac{1}{\beta} \sum_a R_a Q_a - \beta J^2 \Delta^2 \sum_{ab} q_{ab}^2 - \frac{1}{\beta} \sum_{a \neq b} r_{ab} q_{ab} \\ & - \frac{1}{\beta} \ln \int \prod_{\mu a} dm_a^\mu \frac{\beta N}{2\pi} \exp \left(\frac{\beta J}{f(1-f)} \sum_a \tilde{\eta}_i^1 m_a V_i^a - \sum_a R_a V_i^a - \sum_{a \neq b} r_{ab} V_i^a V_i^b \right) \\ & - \frac{\alpha}{\beta} \ln \int \left(\prod_a dm_a \right) \exp \left(-\frac{\beta J}{2f(1-f)} \sum_a m_a^2 + \frac{\beta^2 J^2}{2f(1-f)} \sum_{a \neq b} m_a m_b q_{ab} \right). \end{aligned} \quad (\text{A20})$$

The free energy per neuron is given as

$$G/N = \lim_{n \rightarrow 0} \frac{1}{n} \min g(\beta, m, Q, q, R, r). \quad (\text{A21})$$

In the large N limit, $\min g(\beta, m, Q, q, R, r)$ is dominated by its value at saddle points. Next we will give the saddle point equations using replica symmetric ansatz. We assume that saddle point values of the order parameters are not dependent on their replica index:

$$m_a = m, \quad Q_a = Q, \quad R_a = R, \quad q_{ab} = q, \quad r_{ab} = r \quad (a \neq b). \quad (\text{A22})$$

Now the free energy per neuron is simplified to

$$\begin{aligned} G/N = & \frac{m^2}{2f(1-f)} + \frac{\alpha}{2\beta} \left\{ \ln [1 - \beta J(Q - q)] - \frac{\beta J q}{1 - \beta J(Q - q)} \right\} - \frac{r q}{2\beta} + \frac{R Q}{\beta} + \theta Q - \frac{1}{4} \beta J^2 \Delta^2 (q^2 - Q^2) \\ & - \frac{1}{\beta} \int Dz \ln \left[1 + \exp \left(\frac{\beta J}{f(1-f)} m \tilde{\eta} + R - \frac{r}{2} + \sqrt{r z} \right) \right]. \end{aligned} \quad (\text{A23})$$

The saddle point equations are obtained by setting the derivatives of G/N to 0:

$$\begin{aligned} \frac{m}{f(1-f)} &= \int Dz \left\langle \left\langle \tilde{\eta} K \left\{ \beta \left[\frac{Jm\tilde{\eta}}{f(1-f)} + \frac{1}{\beta} \left(R - \frac{\alpha\beta^2\tilde{r} + \beta^2 J^2 \Delta^2 q}{2} \right) + \sqrt{\alpha\tilde{r} + J^2 \Delta^2 qz} \right] \right\} \right\rangle \right\rangle, \\ R - \frac{\alpha\beta^2\tilde{r} + \beta^2 J^2 \Delta^2 q}{2} &= \frac{\alpha}{2} \frac{\beta(Q-q)J}{1-\beta J(Q-q)} - \beta\theta + \frac{1}{2}\beta^2(Q-q)J^2\Delta^2, \\ \tilde{r} &= \frac{J^2 q}{[p1 - J\beta(Q-q)]^2}, \\ Q &= \int Dz \left\langle \left\langle K \left\{ \beta \left[\frac{Jm\tilde{\eta}}{f(1-f)} + \frac{1}{\beta} \left(R - \frac{\alpha\beta^2\tilde{r} + \beta^2 q}{2} \right) + \sqrt{\alpha\tilde{r} + J^2 \Delta^2 qz} \right] \right\} \right\rangle \right\rangle, \\ q &= \int Dz \left\langle \left\langle K^2 \left\{ \beta \left[\frac{Jm\tilde{\eta}}{f(1-f)} + \frac{1}{\beta} \left(R - \frac{\alpha\beta^2\tilde{r} + \beta^2 q}{2} \right) + \sqrt{\alpha\tilde{r} + J^2 \Delta^2 qz} \right] \right\} \right\rangle \right\rangle, \end{aligned} \quad (\text{A24})$$

where $\tilde{r} = \frac{1}{\beta^2\alpha}(r - \beta^2 J^2 \Delta^2 q)$, $K(x) = [1 + \exp(-x)]^{-1}$, and $Dz = dz \frac{\exp(-x^2/2)}{\sqrt{2\pi}}$. In the zero-temperature limit $\beta \rightarrow \infty$, these saddle point equations can be simplified to

$$\begin{aligned} \tilde{m} &= \Phi(a_1) - \Phi(a_2), \\ \tilde{r} &= f\Phi(a_1) + (1-f)\Phi(a_2), \\ a_1 &= \frac{\tilde{\theta} - (1-f)\tilde{m} - Y}{\sqrt{\tilde{r}\alpha[1 + \Delta_0^2(1-C)^2]}}, \\ a_2 &= \frac{\tilde{\theta} + f\tilde{m} - Y}{\sqrt{\tilde{r}\alpha[1 + \Delta_0^2(1-C)^2]}}, \\ Y &= \frac{\alpha Cf}{2(1-C)} + \frac{1}{2}\alpha Cf\Delta_0^2, \\ C &= \frac{f}{2\pi\alpha\tilde{r}} [f e^{-a_1^2/2} + (1-f)e^{-a_2^2/2}], \end{aligned} \quad (\text{A25})$$

where $\tilde{m} = m/f(1-f)$, $\tilde{\theta} = \theta/f$, $\Delta_0^2 = \Delta^2/\alpha$, and $\Phi(x) = \int_x^\infty Dz$.

3. Sparse coding limit

In the sparse coding limit $f \rightarrow 0$, C goes to zero and Y goes to zero. Equations (A25) become

$$\begin{aligned} \tilde{m} &= \Phi\left(\frac{\tilde{\theta} - \tilde{m}(1-f)}{\sqrt{\tilde{r}\alpha(1 + \Delta_0^2)}}\right) - \Phi\left(\frac{\tilde{\theta} + f\tilde{m}}{\sqrt{\tilde{r}\alpha(1 + \Delta_0^2)}}\right), \\ \tilde{r} &= f\Phi\left(\frac{\tilde{\theta} - f\tilde{m}}{\sqrt{\tilde{r}\alpha(1 + \Delta_0^2)}}\right) + \Phi\left(\frac{\tilde{\theta}}{\sqrt{\tilde{r}\alpha(1 + \Delta_0^2)}}\right). \end{aligned} \quad (\text{A26})$$

In the small f limit, $\tilde{m} \sim 1$ requires

$$\Phi\left(\frac{\tilde{\theta} - \tilde{m}(1-f)}{\sqrt{\alpha f \pi/2}}\right) \sim 1, \quad \Phi\left(\frac{\tilde{\theta} + \tilde{m}f}{\sqrt{\alpha f \pi/2}}\right) \ll 1. \quad (\text{A27})$$

Furthermore, α is maximized when \tilde{r} is minimized, which requires the stronger condition

$$\Phi\left(\frac{\tilde{\theta} + \tilde{m}f}{\sqrt{\alpha f \pi/2}}\right) \ll f, \quad (\text{A28})$$

which leads to $\tilde{r} \sim f$. Using $\lim_{x \rightarrow +\infty} \Phi(x) \simeq \frac{1}{x\sqrt{2\pi}} \exp(-\frac{x^2}{2})$, in the small f limit, Eq. (A28) gives

$$\sqrt{\frac{\alpha f}{2\tilde{\theta}^2}} \exp\left(-\frac{\tilde{\theta}^2}{\pi f \alpha}\right) \ll f. \quad (\text{A29})$$

Rewriting $\alpha = k/f \ln(f^{-1})$, we find that Eq. (A29) is satisfied provided $k < \theta^2/\pi$. Thus, the maximum storage capacity α increases with $\tilde{\theta}^2$ as

$$\alpha_c \simeq \frac{\tilde{\theta}^2}{\pi f |\ln f|}. \quad (\text{A30})$$

In the sparse coding limit, the optimal threshold is obtained at $\tilde{\theta} = 1$ (the maximum value of $\tilde{\theta}$), and thus

$$\alpha_c = \frac{1}{\pi f |\ln f|}. \quad (\text{A31})$$

This storage capacity coincides with the optimal capacity obtained by Gutfreund for the Ising interaction case (see Appendix 4, for details).

We next ask the question of how close the threshold can be to 1, when the coding level f is small but finite. The threshold needs to be sufficiently far from one, so that the argument of the function Φ in the first condition in Eq. (A27) is large and negative. We find that for thresholds that are close to 1, the maximal capacity is

$$\alpha = \frac{(1 - \tilde{\theta})^2}{\pi f |\ln(1 - \tilde{\theta})|}. \quad (\text{A32})$$

Equations (A30) and (A32) give the optimal threshold θ_{opt} (i.e., the optimal value of $\tilde{\theta}$) as a solution to the equation

$$\frac{2\theta_{\text{opt}}^2 |\ln(1 - \theta_{\text{opt}})|}{(1 - \theta_{\text{opt}})^2} = |\ln f|. \quad (\text{A33})$$

The maximum storage capacity is

$$\alpha_c \simeq \frac{\theta_{\text{opt}}^2}{\pi f |\ln f|}, \quad (\text{A34})$$

where θ_{opt} is given as a function of f by Eq. (A33). When $f \rightarrow 0$, $\theta_{\text{opt}} \rightarrow 1$ and Eq. (A34) becomes the Gutfreund bound (A31). However, this convergence is extremely slow, as shown in Fig. 2.

4. Bounds for capacity

Gardner upper bound for networks with continuous weights (GUBC). This bound was calculated by Gardner in 1987 for networks with continuous weights. The upper bound is obtained when the volume of the space of solutions for the weights $\{J_{ij}\}$ vanishes (see details in [4]). By solving Eqs. (37) and (38) in [4], one can obtain the GUBC for arbitrary coding levels. This result is shown by the red curve in Fig. 2.

In the sparse coding limit, the asymptotic solution is given in Eq. (40) in [4], where

$$\alpha_{\text{cmax}} = \frac{1}{2f |\ln f|}. \quad (\text{A35})$$

Gutfreund and Stein upper bound for networks with binary weights (GUBB). This bound was calculated by Gutfreund and Stein in 1990 [14]. They extended Gardner's formalism to the case of networks with binary weights. Using a replica symmetric ansatz, the solution space of binary weights vanishes when capacity reaches

$$\alpha_{\text{cmax}} = \frac{2}{\pi} \text{GUBC}. \quad (\text{A36})$$

In the sparse coding limit, Eqs. (A35) and (A36) give

$$\alpha_{\text{cmax}} = \frac{1}{\pi f |\ln f|}. \quad (\text{A37})$$

However, it can be shown that replica symmetry is broken, and Eq. (A36) is an overestimate. A better estimate of the upper bound for networks with binary weights is given by zero entropy condition (see [14] for details), obtained by solving Eqs. (20)–(24) and (29)–(34) in [14]. This zero entropy line is shown by the blue curve in Fig. 2.

By numerically solving Eqs. (20)–(24) and (29)–(34) in [14] and Eqs. (37) and (38) in [4], one can see that the zero entropy line is getting close to the Gardner line [Eq. (A36)] when the coding level decreases. This numerical result indicates that Eq. (A37) is also a good estimate for the zero entropy line in the sparse coding limit.

5. Storage capacity of the sparsely connected CTF model

Using similar calculations as in Appendix 1, one can obtain that the nonlinear learning rule (17) can be transformed to a linear learning rule:

$$W_{ij} = \frac{c_{ij}}{cNf(1-f)} \sum_{\mu} (\eta_i^{\mu} - f)(\eta_j^{\mu} - f) + \delta_{ij}, \quad (\text{A38})$$

where the variance of $\delta_{ij} = \frac{\alpha \Delta_0^2}{N} = \frac{\alpha}{N} (1 + \frac{\pi}{2})$, and where the connection probability $c \ll 1$. In this case, the local field h_i can be written as

$$h_i = \sum_{i \neq j}^N W_{ij} V_j = \frac{1}{cf(1-f)N} \tilde{\eta}_i^1 \sum_j^N c_{ij} \tilde{\eta}_j^1 V_j + \frac{1}{cf(1-f)N} \sum_{\mu > 1} \sum_j^N c_{ij} \tilde{\eta}_i^{\mu} \tilde{\eta}_j^{\mu} V_j + \sum_j^N \delta_{ij} V_j, \quad (\text{A39})$$

where $\tilde{\eta}_i^1$ denote the pattern that is currently being retrieved by the network. When N and p are large, the second and third terms in the right-hand side of Eq. (A39) Y_1 and follow a Gaussian distribution with zero mean. Introducing order parameters $\tilde{m} = m/f(1-f)$ and q defined in Eq. (19), Eq. (A39) can be simplified to

$$h_i = \tilde{\eta}_i^1 \tilde{m} + Y, \quad (\text{A40})$$

where the variance of Y is

$$\text{var}(Y) = \alpha_s (\Delta_0^2 + 1) q \quad (\text{A41})$$

and $\alpha_s = p/cN$:

$$\tilde{m} = \frac{1}{Nf(1-f)} \sum_j^N \tilde{\eta}_j^1 \Theta(\tilde{\eta}_j^1 \tilde{m} + Y - \theta), \quad (\text{A42})$$

$$q = \frac{1}{N} \sum_j^N \Theta^2(\tilde{\eta}_j^1 \tilde{m} + Y - \theta). \quad (\text{A43})$$

Averaging Eqs. (A42) and (A43) over η and the Gaussian noise Y , the mean-field equations for order parameters \tilde{m} and q are

$$\tilde{m} = \Phi\left(\frac{\tilde{\theta} - \tilde{m}(1-f)}{\sqrt{\alpha_s q (1 + \Delta_0^2)}}\right) - \Phi\left(\frac{\tilde{\theta} + \tilde{m}f}{\sqrt{\alpha_s q (1 + \Delta_0^2)}}\right),$$

$$q = f \Phi\left(\frac{\tilde{\theta} - \tilde{m}(1-f)}{\sqrt{\alpha_s q (1 + \Delta_0^2)}}\right) + (1-f) \Phi\left(\frac{\tilde{\theta} + \tilde{m}f}{\sqrt{\alpha_s q (1 + \Delta_0^2)}}\right). \quad (\text{A44})$$

Note that these equations coincide with the fully connected case in the sparse coding limit, as in the case of continuous weights [2,17].

6. Numerical simulations

The simulations in Fig. 1 used a network with 4000 neurons and coding level $f = 0.02$. The overlaps \tilde{m} are averaged over five independent realizations. Simulations consist in a learning phase in which the connectivity matrix W_{ij} is built, and a retrieval phase in which network dynamics run until it reaches a fixed point. For each input pattern μ , we choose as initial conditions $\{V_i = \eta_i^{\mu}\}$. Overlaps m are obtained by averaging over all m^{μ} .

- [1] J. J. Hopfield, Neural networks and physical systems with emergent collective computational abilities, *Proc. Natl. Acad. Sci. USA* **79**, 2554 (1982).
- [2] M. V. Tsodyks, and M. V. Feigel'man, The enhanced storage capacity in neural networks with low activity level, *Europhys. Lett.* **6**, 101 (1988).
- [3] D. J. Amit, H. Gutfreund, and H. Sompolinsky, Statistical mechanics of neural networks near saturation, *Ann. Phys.* **173**, 30 (1987).
- [4] E. Gardner, The space of interactions in neural network models, *J. Phys. A: Math. Gen.* **21**, 257 (1988).
- [5] C. C. Petersen, R. C. Malenka, R. A. Nicoll, and J. J. Hopfield, All-or-none potentiation at CA3-CA1 synapses, *Proc. Natl. Acad. Sci. USA* **95**, 4732 (1998).
- [6] D. H. O'Connor, G. M. Wittenberg, and S. S-H. Wang, Graded bidirectional synaptic plasticity is composed of switch-like unitary events, *Proc. Natl. Acad. Sci. USA* **102**, 9679 (2005).
- [7] M. Hruska, N. Henderson, S. J. Le Marchand, H. Jafri, and M. B. Dalva, Synaptic nanomodules underlie the organization and plasticity of spine synapses, *Nat. Neurosci.* **21**, 671 (2018).
- [8] S. Dorkenwald, N. L. Turner, T. Macrina, K. Lee, R. Lu, J. Wu, A. L. Bodor, A. A. Bleckert, D. Brittain, N. Kemnitz *et al.*, Binary and analog variation of synapses between cortical pyramidal neurons, *BioRxiv* (2019).
- [9] W. Krauth, and M. Mézard, Storage capacity of memory networks with binary couplings, *J. Phys.* **50**, 3057 (1989).
- [10] H. Sompolinsky, *The Theory of Neural Networks: The Hebb Rule and Beyond, Heidelberg Colloquium on Glassy Dynamics* (Springer, Berlin, 1987).
- [11] H. Sompolinsky, Neural networks with nonlinear synapses and a static noise, *Phys. Rev. A* **34**, 2571 (1986).
- [12] J. S. Lee, J. J. Briguglio, J. D. Cohen, S. Romani, and A. K. Lee, The statistical structure of the hippocampal code for space as a function of time, context, and value, *Cell* **183**, 620 (2020).
- [13] S. Waydo, A. Kraskov, R. Q. Quiroga, I. Fried, and C. Koch, Sparse representation in the human medial temporal lobe, *J. Neurosci.* **26**, 10232 (2006).
- [14] H. Gutfreund and Y. Stein, Capacity of neural networks with discrete synaptic couplings, *J. Phys. A: Math. Gen.* **23**, 2613 (1990).
- [15] M. Mézard, G. Parisi, and M. A. Virasoro, *Spin Glass Theory and Beyond: An Introduction to the Replica Method and Its Applications* (World Scientific, Singapore, 1987), Vol. 9.
- [16] H. Markram, J. Lübke, M. Frotscher, A. Roth, and B. Sakmann, Physiology and anatomy of synaptic connections between thick tufted pyramidal neurones in the developing rat neocortex, *J. Physiol.* **500**, 409 (1997).
- [17] M. V. Tsodyks, Associative memory in asymmetric diluted network with low level of activity, *Europhys. Lett.* **7**, 203 (1988).
- [18] B. Derrida, E. Gardner, and A. Zippelius, An exactly solvable asymmetric neural network model, *Europhys. Lett.* **4**, 167 (1987).
- [19] M. V. Tsodyks, Associative memory in neural networks with binary synapses, *Mod. Phys. Lett. B* **4**, 713 (1990).
- [20] D. J. Amit and S. Fusi, Constraints on learning in dynamic synapses, *Netw., Comput. Neural Syst.* **3**, 443 (1992).
- [21] D. J. Amit and S. Fusi, Learning in neural networks with material synapses, *Neural Comput.* **6**, 957 (1994).
- [22] A. M. Dubreuil, Y. Amit, and N. Brunel, Memory capacity of networks with stochastic binary synapses, *PLoS Comput. Biol.* **10**, e1003727 (2014).
- [23] M. K. Benna and S. Fusi, Computational principles of synaptic memory consolidation, *Nat. Neurosci.* **19**, 1697 (2016).
- [24] S. Lahiri and S. Ganguli, A memory frontier for complex synapses, *NeurIPS* **26**, 1034 (2013).
- [25] S. Fusi, P. J. Drew, and L. F. Abbott, Cascade models of synaptically stored memories, *Neuron* **45**, 599 (2005).
- [26] S. Fusi and L. F. Abbott, Limits on the memory storage capacity of bounded synapses, *Nat. Neurosci.* **10**, 485 (2007).